Journal of
Mechanics of Materials and Structures

FREQUENCY AND SPATIAL RESPONSE OF BASILAR MEMBRANE VIBRATION IN A THREE-DIMENSIONAL GERBIL COCHLEAR MODEL

Yongjin Yoon, Sunil Puria and Charles R. Steele

Volume 2, Nº 8 *October 2007*

mathematical sciences publishers

JOURNAL OF MECHANICS OF MATERIALS AND STRUCTURES
Vol. 2, No. 8, 2007

FREQUENCY AND SPATIAL RESPONSE OF BASILAR MEMBRANE VIBRATION IN A THREE-DIMENSIONAL GERBIL COCHLEAR MODEL

YONGJIN YOON, SUNIL PURIA AND CHARLES R. STEELE

The cochlea of the inner ear presents severe difficulties for measurement and computation, and controversy exists on virtually every issue. However, the first in vivo measurement of the spatial distribution of elastic response for a fixed frequency is now available. This work compares experimental results and those from calculations with a three-dimensional model. This is a standard model that consists of a long, fluid-filled box with a partition, a portion of which is the elastic BM (basilar membrane). The BM velocity at a fixed point as a function of frequency and the spatial response for a fixed frequency are calculated. The model includes the three-dimensional viscous fluid and the pectinate zone of the elastic orthotropic BM with the gerbil dimensional and material property variation along its length. The radial BM thickness variation is, however, replaced by an equivalent constant thickness. The active process is represented by adding the motility of the OHCs (outer hair cells) to the passive model with a feed-forward approximation of the organ of Corti (OC). Asymptotic and numerical methods combined with Fourier series expansions are used to provide a fast and efficient iterative procedure that requires about one second on a desktop computer for obtaining the BM response for a given frequency. Our three-dimensional model results show the following agreement with the experimental measurements in various situations: (i) for map of place of maximum response to frequency — excellent; (ii) for the response at a fixed point as a function of frequency — excellent for amplitude, poor for phase; (iii) for the spatial distribution for fixed frequency — fair for amplitude and excellent for phase. The discrepancies in (ii) and (iii) remain to be clarified.

1. Introduction

The cochlea is a snail-shaped, fluid-filled duct that is divided along its longitudinal direction by the compliant basilar membrane (BM), upon which is located the organ of Corti (OC) containing all sensory cells. The fluid and compliant structures within the cochlea are set in motion in response to sound input at the stapes, and the detection of this motion by inner hair cells (IHCs) initiates hearing through afferent auditory nerve firing transmitted to the auditory cortex. In this study, the mechanical behavior of the cochlea, especially BM velocity, was simulated with a physiologically based, three-dimensional cochlear model. Model results were compared with in vivo cochlear experimental data in the characteristic frequency-to-place (CF-to-place) map and BM velocity magnitude and phase for the frequency and spatial distribution. Access for in vivo measurement in the cochlea is severely restricted and difficult. The first in vivo measurement of the spatial distribution of elastic response for a fixed frequency by Ren [2002] provides the motivation for the present study.

Keywords: cochlear model, mechanical response, basilar membrane velocity, outer hair cell, gerbil.
This work was funded by HFSP Grant No. RGP0051.

Numerous mathematical models describe the biomechanical activity in the cochlea. Models extend the passive cochlear model with the inclusion of the motions of OC, particularly the active behavior of the outer hair cells (OHC), beginning with simplified one-dimensional models with negative damping [de Boer 1983]. Higher-dimensional active models have also been developed. Two-dimensional finite difference models were constructed by using a feedback law [Neely 1985; 1993]. Numerically intense three-dimensional finite-element models had been developed with the inclusion of varying details and complexities of the OC, but the fluid was still modeled as inviscid [Kolston and Ashmore 1996; Böhnke and Arnold 1998]. Models include the activity in the OC as a feed-forward mechanism from the longitudinal tilt of the OHCs. Two-dimensional [Geisler and Sang 1995] and three-dimensional models with the active feed-forward mechanism have been employed [Steele et al. 1993; Steele and Lim 1999; Lim and Steele 2002].

The present study uses the physiologically based, linear three-dimensional feed-forward model for gerbil anatomy. The model uses a combination of the asymptotic phase integral method that is commonly known as WKB (Wentzel–Kramers–Brillouin) method and the fourth order Runge–Kutta (RK4) numerical forward integration. This hybrid approach provides significantly faster computations than the finite difference or finite element methods and more accuracy than the WKB alone [Lim and Steele 2002].

The present model is as simple as possible while still representing the essential features of the BM response. Included in the model are the variation of the dimensions and material properties along the cochlear duct and three-dimensional viscous fluid effects. Only one degree of freedom of the partition, the flexing of the pectinate zone of the orthotropic BM, is considered. The spiral coiling of the cochlea is neglected, as it has been shown to have little effect on the model response [Loh 1983; Steele and Taber 1979]. The simulation results obtained from this active model successfully demonstrate various aspects of in vivo measurements. Since it is difficult to understand the dynamic response of a structure from measurements alone, particularly when the measurements are restricted to a few locations along the cochlea, a reliable model and calculation procedure plays an important role.

2. Mathematical methods

2.1. ***Passive model.*** The physical cochlea consists of a rigid bony housing containing two coiled, fluid-filled ducts, separated by the cochlear partition. The model is based on these physiologic features of the cochlea. A schematic drawing of the model with the side, cross-section, and top view is shown in Figure 1. The detailed derivations and features for the passive mechanics were described in a previous study [Lim and Steele 2002]. Briefly, the three-dimensional fluid equations are integrated over the cross-section to obtain the relation between the volume flow and the fluid pressure at the BM. Then the fluid impedance is matched to the elastic BM impedance, which yields the second order reduced wave equation

$$G_{,xx} + n(x,\omega)^2 G = 0, \tag{1}$$

in which $n(x,\omega)$ is the local wave number, determined from an *eikonal* equation dependent on distance x and frequency ω. The eikonal equation is complex valued, dependent on the Fourier series expansions on the cross-section of the three-dimensional viscous fluid. An iterative solution for n is obtained at each x for fixed ω. The form of the x-dependence is not assumed *a priori*, but comes from the solution of

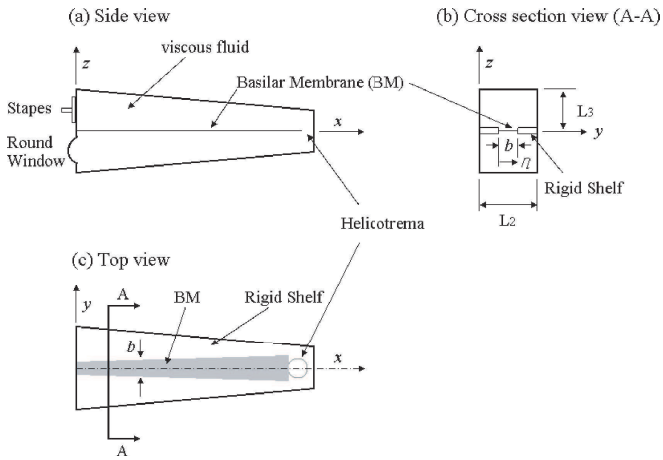

Figure 1. Schematic drawing of the passive cochlear model geometric layout. Distances parameterized in Cartesian coordinates $\{x, y, z\}$ representing distance from stapes, distance across scala width, and height above partition, respectively. (a) Side, (b) cross-section (A-A), and (c) top views of cochlear model.

Equation (1). The dependent variable $G(x)$ provides the potential $\Phi(x)$ for the fluid,

$$\Phi(x) = \frac{G(x)n}{T_0 \sinh(nL_3)},$$

where $T_0(x)$ is the Fourier coefficient for the 0-th component of scalar potential for fluid displacement, and L_3 is the height of fluid chamber.

The function $G(x)$ is obtained from Equation (1) by using the well-known WKB asymptotic solution in the short wavelength region (n large) and the RK4 forward integration in the long wavelength region (n small). The boundary conditions of matching the volume displacement at the stapes and zero pressure at the helicotrema are taken into account with forward and reverse traveling waves.

2.2. ***Feed-forward active model.*** The active elements in the cochlea are the OHCs which behave as piezoelectric actuators. In this model, the force applied by the OHCs on the BM partition is assumed to be proportional to the total force acting on the BM. The total force at the pectinate zone (PZ) results from the fluid force difference across the two scala and forces resulting from the OHCs motility,

$$F_{PZ} = 2F_{BM}^{f} + F_{BM}^{C}. \tag{2}$$

The OHC force acting at $x + \Delta$ is proportional to the BM displacement sensed at x by the effect of the OHC longitudinal tilt as in Figure 2, or

$$F_{BM}^{C}(x + \Delta) = \alpha(x) F_{PZ}(x), \tag{3}$$

where α is the feed-forward gain factor and Δ is the longitudinal distance between the apex and base of the OHC, which depends on the length of the OHC l_{OHC} and its angle with respect to the longitudinal direction θ, via $\Delta = l_{OHC} \cos\theta$. Combining Equations (2) and (3) provides a modification of the eikonal equation keeping the same form of the equation for G Equation (1) [Lim and Steele 2002].

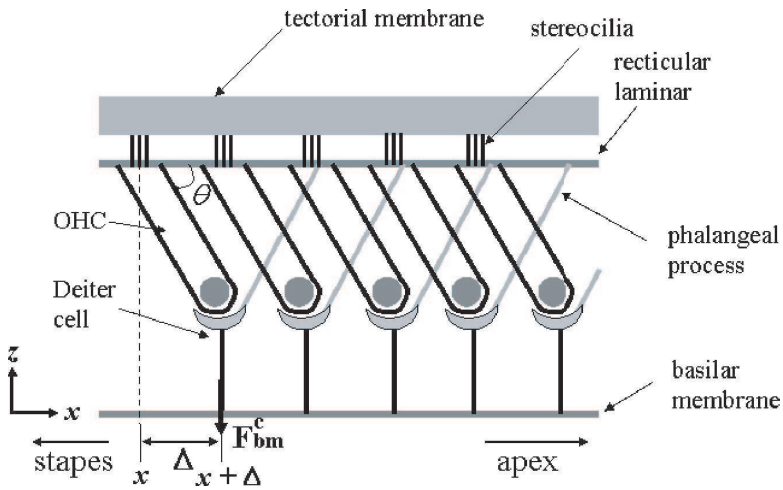

Figure 2. Schematic of longitudinal view of OC, showing longitudinal tilt of OHC. Longitudinal distance between base and apex of OHC is defined as Δ.

3. Results and discussion

The cochlear model is used to calculate the response of a gerbil cochlea. The material property values in Table 1 were taken from a number of sources [Smith 1968; Lim and Steele 2002; Miller 1985; Steele et al. 1995; Karavitaki 2002] and the dimensions in Table 2 were from the anatomical measurements for gerbil cochlea [Sokolich et al. 1976; Greenwood 1990; Dannhof et al. 1991; Cohen et al. 1992; Edge et al. 1998; Thorne et al. 1999].

The model is meshed into 12000 sections along the gerbil cochlea length of 12 mm. Forty terms are used in the Fourier expansion across the width of the cross-section. Running on an Intel Pentium IX 3.40 GHz processor, the average time taken for a single harmonic excitation calculation is about one second. This method is a fast and efficient solution compared to a full-scale finite element model. We

Basilar membrane	$E_{11} = 1.0 \times 10^{-3}$ GPa $E_{22} = 1.0$ GPa $E_{12} = 0.0$ GPa $\rho_p = 1.0 \times 10^3$ kg/m^3 $\nu = 0.5$
Scala fluid	$\rho_f = 1.0 \times 10^3$ kg/m^3 $\mu = 0.7 \times 10^{-3}$ Pa s
Outer hair cell	$\theta = 60°$ and $80°$ $\alpha = 0.17$

Table 1. Gross properties in cochlear model.

x (mm)	b (mm)	h (mm)	f	L_2, L_3 (mm)	l_{OHC} (μm)
0		0.0210	0.030	1.000	25.0
1.5		0.0175			
2.9	0.162			0.750	
3.5		0.0131			
5.0				0.480	
5.9		0.0088			
7.2	0.190	0.0073		0.370	
8.4					
9.0		0.0055		0.340	
10.2	0.205	0.0044			
12.0		0.0031	0.007	0.310	65.0

Table 2. Property variations in gerbil cochlear model: b, h and f are width, thickness and fiber density of plate, respectively; L_2, L_3 are width and height of fluid chamber; l_{OHC} is OHC length. The thickness h is not anatomical but an equivalent value to give proper tuning.

note that the computation time indicated by Parthasarathi et al. [2000] is measured in hours of computing time for the linear solution for a single frequency.

The results include CF-to-place map for the gerbil cochlea, BM velocity frequency response, and BM velocity spatial response. The modeling results for the gerbil cochlea are compared with recent in vivo experiment measurements in the cochlea.

3.1. ***CF-to-place map.*** CF versus distance from the stapes along the gerbil cochlear (CF range: 0.3 kHz–50 kHz) is shown in Figure 3. The gerbil CF-to-place map [Sokolich et al. 1976; Greenwood 1990] was measured with cochlear-microphonic recording. The maps from the passive model and measurement are in excellent agreement; see Figure 3. Near the stapes (0–4 mm from the stapes), the active model shows 4.5 dB CF shift, whereas CF shift disappears near the helicotrema. Due to the lower wave number for the low input frequency, which has a peak near the apical region of the cochlea, feed-forward gain from the active model shows less gain near the helicotrema.

3.2. ***Frequency response of BM velocity.*** The gerbil cochlear BM velocity magnitude and phase for 4.2 mm from the base ($CF = 9.5$ kHz) relative to the stapes displacement are computed over a range of excitation frequencies up to 18 kHz; see Figure 4. Results from the model are compared with the gerbil experimental data [Ren and Nuttall 2001]. The passive model shows quantitatively very good agreement with data which are measured at a high stimulus level (100 dB SPL at the ear canal).

Karavitaki [2002] gives the angle of tilt of gerbil OHC as $\theta = 84°$, closer to perpendicular to the basilar membrane; see Figure 2. We calculated the gain from OHC for two cases; a nominal mammalian value of $\theta = 60°$ and $\theta = 80°$. The active model shows fairly good agreement with data at low stimulus level (30 dB SPL at the ear canal) with 27 dB gain for either $\theta = 60°$ with feed-forward gain factor $\alpha = 0.15$ (solid-red in Figure 4) or $\theta = 80°$ with forward gain factor $\alpha = 0.28$ (solid-brown). So only a slightly

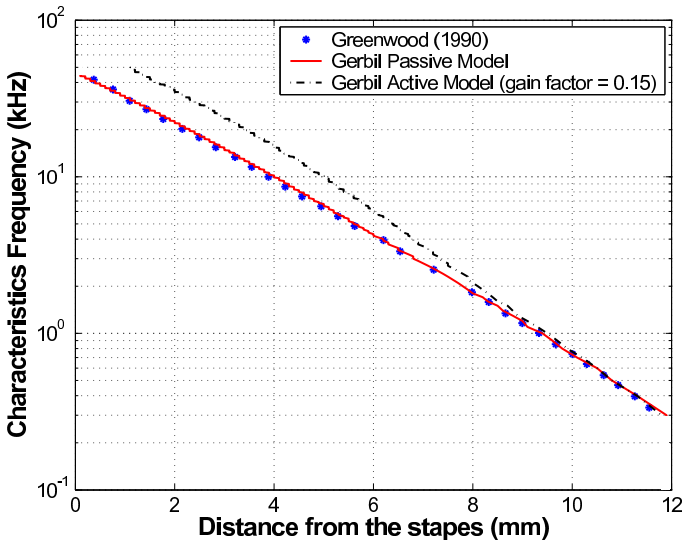

Figure 3. CF versus position for passive cochlear model (solid) compared to measurements (*) and active cochlear model (dashed-dot). Present three-dimensional model represents cochlear CF-to-place map of gerbil [Sokolich et al. 1976; Greenwood 1990] over 0.3–50 kHz range spanning a length of 12 mm.

higher gain, still in the physiologically reasonable range, is needed for the OHC nearly perpendicular to the BM.

In the relative BM velocity magnitude plot (top of Figure 4), CF place shifts from 9.5 kHz (passive model) to 15 kHz (active model), which is 3/5 octave higher. In the animal measurement CF is also near 9.5 kHz for the high level passive case. For the low level active case, CF place shifts to about 13 kHz, which is only about 2/5 octave higher. So the model appears to overestimate the CF for the active case.

In the model, the phase is normalized to the volume flow rate at $x = 0$, as the stapes is assumed to be a piston at the end of the fluid chamber. As shown in the bottom of Figure 4, the phase of the response obtained from the model shows a larger roll-off with frequency than the experimental measurements. In the region of the low frequency input, below 4 kHz, the BM velocity phases both from the model and measurement are similar. However, after 4 kHz, the phase of BM velocity from the model shows a larger roll-off than the phase from the data, which means over fluctuation in the model above 4 kHz excitation frequency range. To match the phase from the model to the measurement, the phase at 2.8 mm from the stapes (CF of 15 kHz for the passive case) gives the same phase accumulation (magenta dashed-dot line in the bottom of Figure 4) as the data. The actual position of the stapes in the cochlea extends over a small portion of the basal end of the scala vestibuli, which may result in this discrepancy in the phase.

3.3. ***Spatial response of BM velocity.*** Ren [2002] measured the waveform of cochlear partition vibration along the cochlear partition from the gerbil cochlea in vivo by using a scanning laser interferometer. In this measurements, he could successfully obtain a *snapshot*, that is, the instantaneous waveform of the cochlear partition vibration, for 16 kHz tones in a longitudinal region of the BM (2200–3000 μm from the stapes). In Figure 5, instantaneous waveforms and BM velocity phase for the passive case are presented.

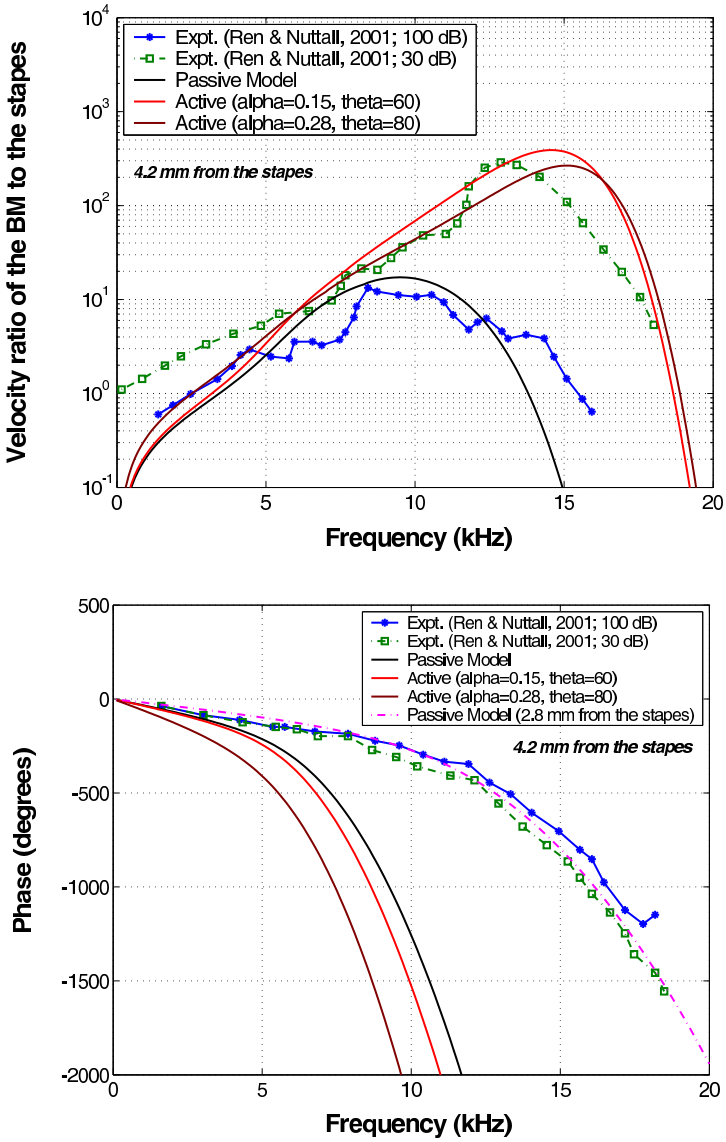

Figure 4. BM velocity relative to the stapes: (top) magnitude and (bottom) corresponding phase for the gerbil cochlea at 4.2 mm from the base ($CF = 9.5$ kHz). For active model, 0.15 feed-forward gain factor α for $\theta = 60°$ (solid-red) and 0.28 feed-forward gain factor for $\theta = 80°$ (solid-brown) was used. Experimental data included for comparison [Ren and Nuttall 2001].

Envelope (magnitude) of the waveform from the model shows less sharp than envelope of the waveform from the measurements; see top of Figure 5. However, the peak place from the model is identical to the measurement (near 2550 μm from the stapes). The snapshot and phase of the waveform from the model shows good agreement with experimental measurement. Around 16 kHz (CF at 2550 μm from the

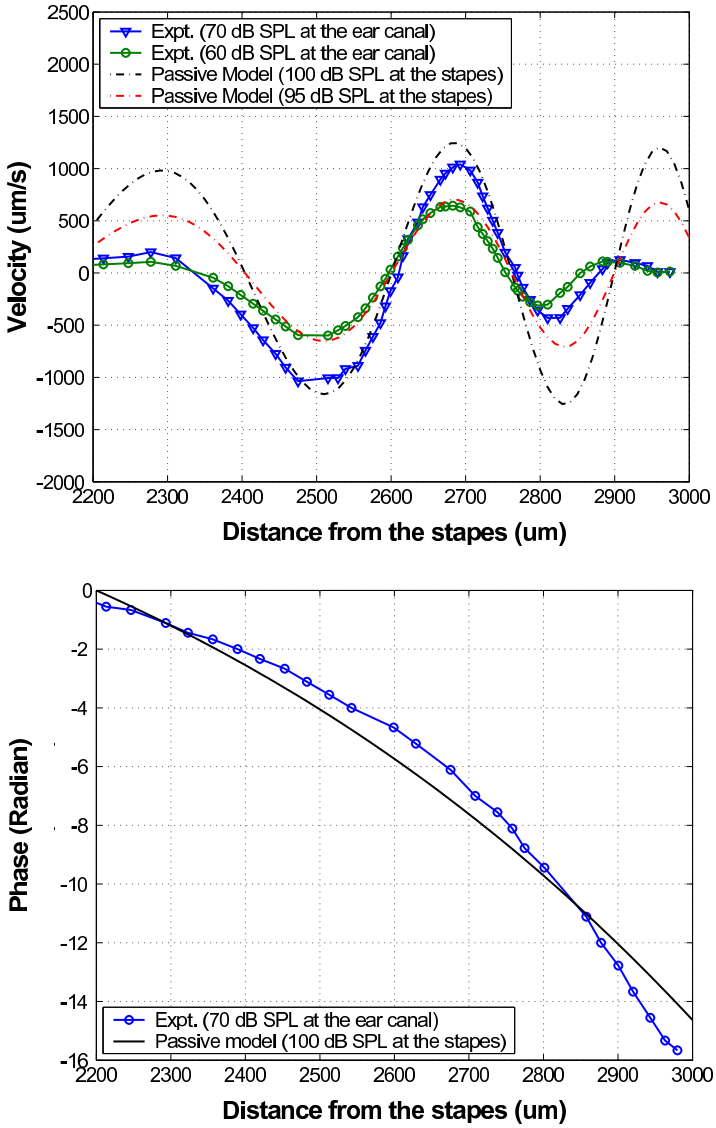

Figure 5. Longitudinal patterns of the instantaneous waveform (top) and phase (bottom) of the BM velocity from passive model and measurements [Ren 2002] near the CF location ($\sim 2550\,\mu$m). Data (70 dB and 60 dB SPL at the ear canal) collected with 16 kHz tones for sensitive gerbil cochlea. Considering 30 dB middle ear gain [Olson 1998], 100 dB and 95 dB SPL at the stapes are used as input pressure in the model, respectively.

stapes), instantaneous waveforms in the model also show energy propagation along the BM, supporting the existence of the cochlear traveling wave on the BM, which was observed in the in vivo measurements; see top of Figure 5. As shown in the bottom of Figure 5, BM velocity phase for the passive model shows around 5 radians delay at the CF for 16 kHz and the total phase delay is around 18 radians ($\sim 6\pi$) over the observed range as in the measurement. Unlike the total phase change of the traveling wave in human

cadavers, which is about 3π radians [Békésy 1960], the phase delay in the gerbil model and measurement is as much as 6π radians over a spatial range of 1000 μm from the stapes.

4. Conclusions

Measurements of the spatial distribution of the response of the BM at a fixed frequency [Ren 2002] and the frequency distribution at a fixed point [Ren and Nuttall 2001] offer an unusual opportunity for validation of model calculations. The macromechanical cochlear model is a simplified box with three-dimensional fluid and geometry from the gerbil anatomy. The BM properties are physical, with orthotropic elastic properties and no fictitious mass or damping. Hence there are no parameters to adjust to fit experimental results.

The comparison of results from the model and experiment is promising, but not fully satisfactory. Using a single set of anatomically based parameters, the model predicts several significant features of cochlear response. The CF-to-place map in the passive model, frequency and spatial responses of BM velocity were in close agreement with those observed in animal measurement. The feed-forward linear active model, the most speculative feature of the framework presented, showed excellent agreement with experimental data in the BM relative velocity magnitude. However, the calculated phase shows excellent agreement for the spatial distribution for fixed frequency, but a much larger roll-off for the frequency dependence at a fixed point. In contrast, the calculated amplitude shows excellent agreement for the fixed point and not quite as sharp a roll-off for the spatial distribution. These limitations in our current model could be resolved by including more detailed structures of the organ of Corti to the current model [Steele and Puria 2005].

References

[Békésy 1960] G. Békésy, *Experiments in hearing*, McGraw-Hill series in psychology, McGraw-Hill, New york, 1960.

[de Boer 1983] E. de Boer, "On active and passive cochlear models-towards a generalized analysis", *J. Acoust. Soc. Am.* **73**:2 (1983), 574–576.

[Böhnke and Arnold 1998] F. Böhnke and W. Arnold, "Nonlinear mechanics of the organ of Corti caused by Deiters cells", *IEEE T. Bio-med. Eng.* **45**:10 (1998), 1227–1233.

[Cohen et al. 1992] Y. E. Cohen, C. K. Bacon, and J. C. Saunders, "Middle ear development, III : morphometric changes in the conducting apparatus of the Mongolian gerbil", *Hearing Res.* **62**:2 (1992), 187–193.

[Dannhof et al. 1991] B. J. Dannhof, B. Roth, and V. Bruns, "Length of hair cells as a measure of frequency representation in the mammalian inner ear", *Naturwissenschaften* **78**:12 (1991), 570–573.

[Edge et al. 1998] R. M. Edge, B. N. Evans, M. Pearce, R. C. P., X. Hu, and P. S. Dallos, "Morphology of the unfixed cochlea", *Hearing Res.* **124**:1-2 (1998), 1–16.

[Geisler and Sang 1995] C. D. Geisler and C. Sang, "A cochlear model using feed-forward outer-hair-cell forces", *Hearing Res.* **86**:1-2 (1995), 132–146.

[Greenwood 1990] D. D. Greenwood, "A cochlear frequency-position function for several species-29 years later", *J. Acoust. Soc. Am.* **87**:6 (1990), 2592–2605.

[Karavitaki 2002] K. D. Karavitaki, *Measurements and models of electrically-evoked motion in the gerbil organ of Corti*, Ph.D. Thesis, MIT, 2002, Available at http://hdl.handle.net/1721.1/8087.

[Kolston and Ashmore 1996] P. J. Kolston and J. F. Ashmore, "Finite element micromechanical modeling of the cochlea in three dimensions", *J. Acoust. Soc. Am.* **99**:1 (1996), 455–467.

[Lim and Steele 2002] K. M. Lim and C. R. Steele, "A three-dimensional nonlinear active cochlear model analyzed by the WKB-numeric method", *Hearing Res.* **170**:1-2 (2002), 190–205.

[Loh 1983] C. H. Loh, "Multiple scale analysis of the spirally coiled cochlea", *J. Acoust. Soc. Am.* **74**:1 (1983), 95–103.

[Miller 1985] C. E. Miller, "Structural implications of basilar membrane compliance measurements", *J. Acoust. Soc. Am.* **77** (1985), 1465–1474.

[Neely 1985] S. T. Neely, "Mathematical modeling of cochlear mechanics", *J. Acoust. Soc. Am.* **78**:1 (1985), 345–352.

[Neely 1993] S. T. Neely, "A model of cochlear mechanics with outer hair cell motility", *J. Acoust. Soc. Am.* **94**:1 (1993), 137–146.

[Olson 1998] E. S. Olson, "Observing middle and inner ear mechanics with novel intracochlear pressure sensors", *J. Acoust. Soc. Am.* **103**:6 (1998), 3445–3463.

[Parthasarathi et al. 2000] A. A. Parthasarathi, K. Grosh, and A. L. Nuttall, "Three-dimensional numerical modeling for global cochlear dynamics", *J. Acoust. Soc. Am.* **107**:1 (2000), 474–485.

[Ren 2002] T. Ren, "Longitudinal pattern of basilar membrane vibration in the sensitive cochlea", *PNAS* **99**:26 (2002), 17101–17106.

[Ren and Nuttall 2001] T. Ren and A. L. Nuttall, "Basilar membrane vibration in the basal turn of the sensitive gerbil cochlea", *Hearing Res.* **151**:1-2 (2001), 48–60.

[Smith 1968] C. A. Smith, "Ultrastructure of the organ of Corti", *Adv. Sci.* **24**:122 (1968), 419–433.

[Sokolich et al. 1976] W. G. Sokolich, R. P. Hamernik, J. J. Zwisiocki, and R. A. Schmiedt, "Inferred response polarities of cochlear hair cells", *J. Acoust. Soc. Am.* **59**:4 (1976), 963–974.

[Steele and Lim 1999] C. R. Steele and K. M. Lim, "Cochlear model with three-dimensional fluid, inner sulcus and feed-forward mechanism", *Audiol. Neuro-Otol.* **4** (1999), 197–203.

[Steele and Puria 2005] C. R. Steele and S. Puria, "Force on inner hair cell cilia", *Int. J. Solids Struct.* **42**:21-22 (2005), 5887–5904.

[Steele and Taber 1979] C. R. Steele and L. A. Taber, "Comparison of WKB calculations and experimental results for three-dimensional cochlear models", *J. Acoust. Soc. Am.* **65**:4 (1979), 1007–1018.

[Steele et al. 1993] C. R. Steele, G. Baker, J. Tolomeo, and D. Zetes, "Electro-mechanical models of the outer hair cell", pp. 207–215 in *Proc. int. symp. biophysics of hair cell sensory systems*, edited by H. Duifhuis et al., World Scientific, Singapore, 1993.

[Steele et al. 1995] C. R. Steele, G. Baker, J. Tolomeo, and D. Zetes, "Cochlear mechanics", pp. 505–516 in *The biomedical engineering handbook*, edited by Z. D. Bronzino, CRC press, 1995.

[Thorne et al. 1999] M. Thorne, A. N. Salt, J. E. DeMott, M. M. Henson, O. W. Henson Jr., and S. L. Gewalt, "Cochlear fluid space dimensions for six species derived from reconstructions of three-dimensional magnetic resonance images", *Laryngoscope* **109**:10 (1999), 1661–1668.

Received 20 Jul 2006. Revised 17 Apr 2007. Accepted 20 Apr 2007.

YONGJIN YOON: yongjiny@stanford.edu
Mechanics and Computation Division, Stanford University, 496 Lomita Mall, Durand Building, Stanford, CA 94305-4035, United States

SUNIL PURIA: puria@stanford.edu
Department of Otolaryngology — Head and Neck Surgery, Stanford University, Stanford, CA 94305, United States

CHARLES R. STEELE: chasst@stanford.edu
Mechanics and Computation Division, Stanford University, 496 Lomita Mall, Durand Building, Stanford, CA 94305-4035, United States